Buoyant mixing of miscible fluids in tilted tubes

T. Séon, J.-P. Hulin,[a] and D. Salin
Laboratoire Fluides Automatique et Systèmes Thermiques, UMR 7608, CNRS, Universités P. et M. Curie and Paris Sud, Bâtiment 502, Campus Universitaire, 91405 Orsay Cedex, France

B. Perrin
Laboratoire Pierre Aigrain, UMR 8551, CNRS, Ecole Normale Supérieure, Département de Physique, 24 rue Lhomond, 75231 Paris Cedex 05, France

E. J. Hinch
DAMTP-CMS, University of Cambridge, Wilberforce Road, CB3 0WA Cambridge, United Kingdom

(Received 27 May 2004; accepted 1 September 2004; published online 21 October 2004)

Buoyant mixing of two fluids in tubes is studied experimentally as a function of the tilt angle θ from vertical, the density contrast and the common viscosity μ. At high contrasts and low θ, longitudinal mixing is macroscopically diffusive, with a diffusivity D increasing strongly with θ and μ. At lower contrasts and higher θ, a counterflow of the two fluids with little transverse mixing sets in. The transition occurs at an angle increasing with density contrast and decreasing with μ. These results are discussed in terms of the dependence of transerse mixing on θ and an analogy with the Boycott effect. © *2004 American Institute of Physics*. [DOI: 10.1063/1.1808771]

Gravity induced mixing of miscible fluids in confined vertical or tilted tube geometries is a widespread phenomenon encountered both in chemical[1,2] and in petroleum engineering. For tubes close to vertical, mixing results from the development of Rayleigh–Taylor instabilities.[3] However, in contrast with many studies of the early phases of these instabilities,[4,5] this paper is concerned with longer times when the mixing occurs over distances much larger than the tube diameter. Closer to horizontal, these processes have many similarities with gravity currents:[6–9] these are, however, often studied in unconfined geometries[6,8] or with little mixing.[7]

The purpose of the present Letter is to analyse the mixing of two fluids of different densities ρ_1 and ρ_2 but with the same viscosity μ in a long tube that can be tilted at angles θ between 0 and 90° from vertical. The density contrast is characterized by the Atwood number $\mathrm{At}=(\rho_2-\rho_1)/(\rho_2+\rho_1)=\Delta\rho/(\rho_2+\rho_1)$.

In our previous work,[10] we investigated experimentally the case of a vertical tube: at high density contrasts, the mixing zone spreads diffusively. The corresponding macroscopic diffusion coefficient D varies slowly with the Atwood number At. An unexpected feature is the increase of D with the fluid viscosity μ. Both results are explained by buoyancy forces depending on the local density contrast $\delta\rho$ that, in turn, depends strongly on the mixing efficiency of the flow. At very low density contrasts, the process is no longer diffusive and one observes a stable counterflow of the two fluids.

In a tilted tube one may expect processes similar to the Boycott effect in the sedimentation of solid particles.[11,12] Particles denser than the fluid gather as sediment in the lower part of the tube section while the fluid is almost clear in the upper part. There then appears a counterflow of the clear fluid and the settling of the suspension speeds up drastically. In the experiments with two fluids described below, both the fluid distribution in the tube section and the mixing process strongly depend on θ (Fig. 2): as in the Boycott effect, the segregation is induced by the transverse gravity component.

In the following, we identify the various flow regimes and their dependence on θ. We focus then on the diffusive regime and analyze the dependence of the macroscopic diffusion coefficient D on θ, At and μ.

Experiments are performed in a long ($L=4$ m) perspex tube of internal diameter $d=20$ mm, with a sliding gate in the middle, that can be tilted at angles θ from 0 to 90° (Fig. 1). The setup is illuminated from behind. The lighter fluid is water dyed with nigrosine (40 mg/l) and the heavy one is a solution of water and $CaCl_2$ salt: At varies from 4×10^{-5} to 3.5×10^{-2}. The viscosities of the two fluids are equal and may be varied between 1 and 4×10^{-3} Pa·s by adding glycerol to both of them. At the beginning of each experiment, the upper and lower halves of the tube are filled, respectively, with the heavy and light solutions; the gate is then opened in a few tenths of a second and measurements are taken during 300–1200 s.

Figure 2 displays video recordings of the 300 mm long section of the tube just above the gate for the three different angles $\theta=0°$, 30°, and 80° and the same density contrast. In these images, one views the mixing zone propagating upwards while there is a symmetrical downwards propagation below the gate (out of view). For the vertical tube, the flow is weakly turbulent and induces an efficient mixing of the two fluids across the tube section.[10] As a result, the boundary of the mixing zone is fuzzier for the vertical tube than for $\theta=30°$ and 80° [Figs. 2(b) and 2(c)].

For $\theta=30°$ [Fig. 2(b)], the displacement front is initially asymmetrical with the lighter (dyed) fluid moving preferentially near the top of the tube section. Behind this front, pseudo-interfacial Kelvin–Helmholtz instabilities develop

[a]Author to whom correspondence should be addressed. Telephone: 33 1 69 15 80 62. Fax: 33 1 69 15 80 60. Electronic mail: hulin@fast.u-psud.fr

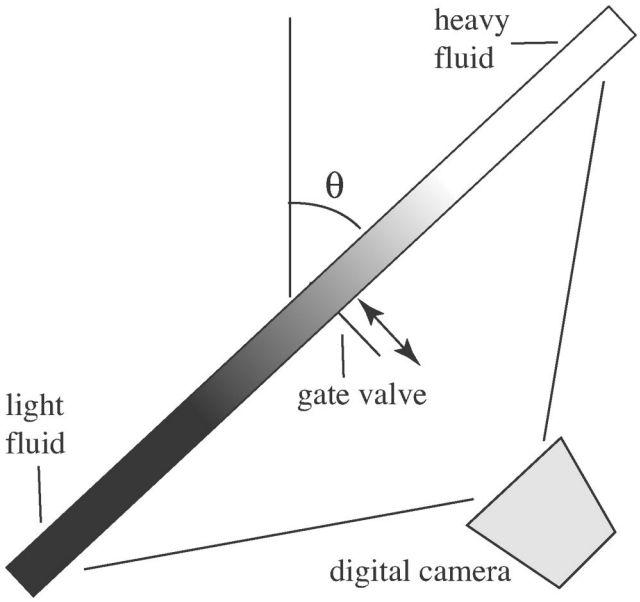

FIG. 1. Schematic view of experimental setup.

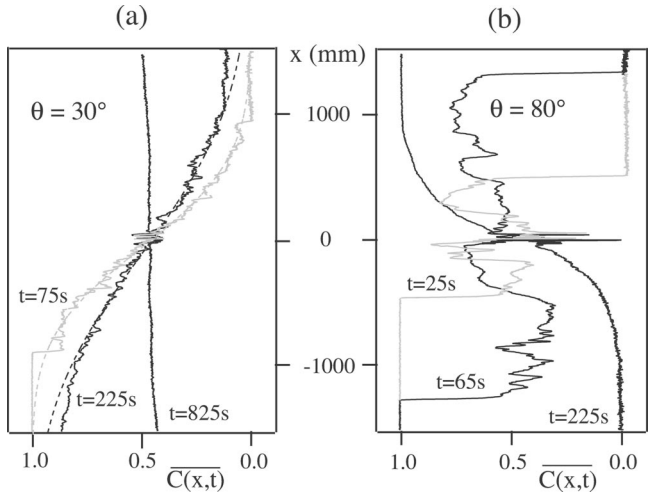

FIG. 3. Variations of $\overline{C(x,t)}$ with distance from gate for $\mathrm{At}=4\times10^{-3}$. (a) At times $t=75$ s (gray curve), 225 s, and 825 s for $\theta=30°$ (dashed lines are fits of the corresponding profile with an error function); (b) at $t=25$ s (gray curve), 65 s, and 225 s for $\theta=80°$.

and mix the two fluids transversally across the section. For $\theta=80°$ [Fig. 2(c)], the two fluids remain almost separate: an initial front with some waves is followed by a parallel counterflow with occasional perturbations of the interface. In this case, the perturbations induce little mixing between the two fluids. Note that the front velocity increases with θ (see Fig. 2).

More quantitative results are obtained by recording with a digital camera images of the 2.5 m long central section of the tube (1300×20 pixels) at 0.5–2 s intervals. These images are then converted into concentration maps normalized by the heavy and light solutions. Pixel values corresponding to the same distance x from the gate are then averaged to obtain the mean concentration $\overline{C(x,t)}$ in the tube section at time t. Concentration profiles $\overline{C(x,t)}$ obtained at different times for the experiments of Figs. 2(b) and 2(c) are displayed in Figs. 3(a) and 3(b).

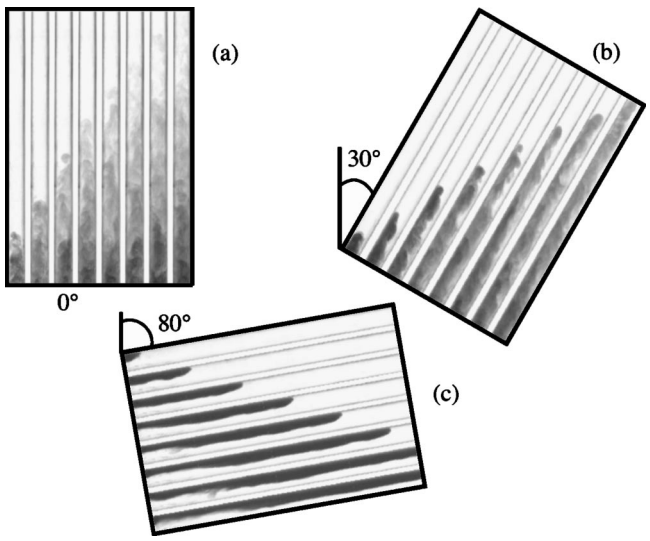

FIG. 2. Snapshots of video images obtained for $\mathrm{At}=4\times10^{-3}$. (a) $\theta=0°$, time interval between images $\Delta t=7$ s. (b) $\theta=30°$, $\Delta t=3$ s. (c) $\theta=80°$, $\Delta t=3$ s.

For moderate angles θ and sufficiently large At, the mean concentration profiles are well fitted by a solution of the classical diffusion equation corresponding to a macroscopic diffusion coefficient D. Until the mixing zone reaches the end of the tube, one can assume that diffusion occurs in an infinite medium and these solutions are error functions [dashed lines in Fig. 3(a)]. As for vertical tubes,[10] mixing results from motions of the two fluids and D is many orders of magnitude larger than the molecular diffusion coefficient. At long times, one reaches a final state that will be discussed later.

For very large θ, the profiles of Fig. 3(b) are no longer diffusive, even at short times. The two fluids remain separated and $\overline{C(x,t)}$ corresponds to the relative fraction of the section occupied by the two fluids and not to the concentration of a mixture. The large fluctuations on the curves reflect therefore perturbations of the interface.

Figure 4(a) displays variations of the measured diffusivity D with $\sin\theta$ in the diffusive regime for several values of At: $\sin\theta$ has been chosen as the control parameter instead of θ since the transverse gravity component $g\sin\theta$ is the driving force inducing segregation. A striking result is the very fast increase of the coefficient D with θ: a factor of 50 between $\theta=0°$ and 70° for $\mathrm{At}=3.5\times10^{-2}$. On the other hand, as also observed for vertical tubes,[10] the dependence of D on At is always weak: for instance, at $\theta=40°$, D increases only by 30% when At increases from 4×10^{-3} to 3.5×10^{-2}.

For a given At, D can only be determined up to a critical angle above which counterflow occurs [Fig. 3(b)]. The value of $\sin\theta$ corresponding to this transition increases strongly with At as can be seen in the flow regime map of Fig. 5(a).

Another important parameter is the fluid viscosity: variations of the diffusion coefficient D with $\sin\theta$ are displayed in Fig. 4 for the same Atwood number ($\mathrm{At}\simeq10^{-2}$) and three different viscosities $\mu=1,2$ and 4×10^{-3} Pa·s. For a given θ,

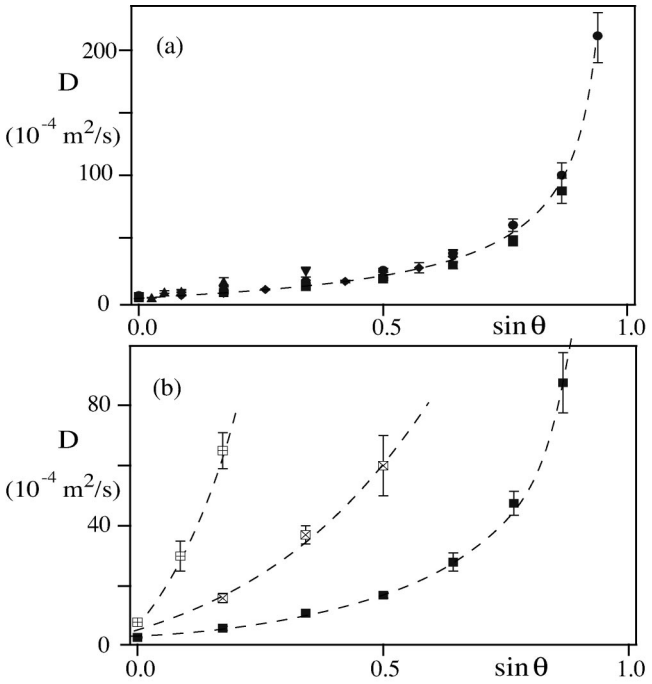

FIG. 4. Variations of the measured diffusivity D with $\sin\theta$. (a) For the same viscosity $\mu=10^{-3}$ Pa·s and for density contrasts: (•): At$=3.5\times10^{-2}$, (■): 10^{-2}, (◆): 4×10^{-3}, (▼): 10^{-3}, (▲): 4×10^{-4}. (b) For the same density contrast At$=10^{-2}$ and for viscosities: (■): $\mu=10^{-3}$ Pa·s, (⊠): 2×10^{-3} Pa·s, (⊞): 4×10^{-3} Pa·s. Dashed lines are provided as guides to the eyes.

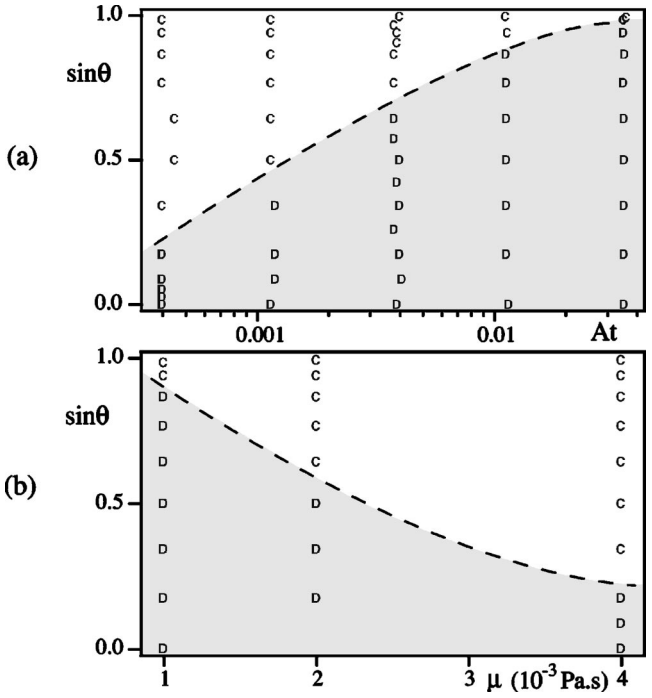

FIG. 5. Flow regime maps displaying the observation of diffusive (D and gray shade) and counterflow (C) mixing regimes in tilted tubes: (a) $\sin\theta$ vs Atwood number At for the same viscosity ($\mu=10^{-3}$ Pa·s); (b) $\sin\theta$ vs the viscosity μ of both fluids (At$=10^{-2}$).

D increases markedly with μ: such an increase is also observed in vertical tubes but it is stronger for tilted ones. The diffusivity D increases roughly as $\mu^{3/2}$ for $\theta\geqslant5°$ instead of μ for a vertical tube.[10] Increasing the viscosity also reduces the range of tilt angles corresponding to diffusive mixing [Fig. 5(b)]: counter flow occurs for instance for θ as low as 10° for $\mu=4\times10^{-3}$ Pa·s.

A key factor to take into account in explaining the variations of the diffusivity D with θ is the transverse gravity component $g\sin\theta$ which induces segregation in the section: the lighter fluid tends to migrate towards the top of the tube section and the heavier one towards the bottom. There results an upwards flow of lighter fluid along the upper side of the tube, and symmetrically a downwards flow of heavier fluid along the lower side. Diffusive spreading of the concentration profile requires transverse mixing between these two flow components through instabilities originating in the center part of the section. Basically, the diffusion coefficient can be estimated as $D\simeq U\times\ell$ where ℓ represents a characteristic distance travelled for transverse exchange and U a characteristic velocity in the upper or lower part of the section. Picturing the process as a random sequence of independent steps, U is the velocity during each step and ℓ its length.

Increasing θ helps to keep the two fluids segregated by increasing buoyancy forces *transverse* to the tube axis. This dampens Kelvin–Helmholtz-like instabilities and reduces transverse mixing.[13] As a result, the path length ℓ increases and so does the mean density contrast $\delta\rho$ between the upper and lower parts of the tube section. Since these flows are controlled by a balance between inertia and buoyancy forces, their typical velocity U is of the order of $(\delta\rho g d)^{1/2}$: U therefore increases also with θ. All these effects contribute to enhance the value of D and are likely to account for the fast variation observed in Fig. 4. Increasing the viscosity μ acts in the same direction: it stabilizes flow in the central part of the pipe and also reduces the Reynolds number, and therefore reduces the efficiency of mixing at small length scales. At very large θ values (or high viscosities), however, the two fluids remain separated in the stable counterflow regime and ℓ becomes of the order of the tube length. Then, the diffusive regime cannot be reached and the spreading of the interpenetration zone is purely convective.

Another issue is the final distribution of the fluid inside the tube [see, for instance, the concentration profiles at $t=825$ s and $t=225$ s, respectively, in Figs. 3(a) and 3(b)]. For tilted tubes and at long times, the final mean concentration gradient is zero or stabilizing (the fluid is then almost motionless). The time necessary to reach this state decreases as θ increases. The final configuration is determined both by the degree of transverse mixing during the interpenetration of the two fluids and by end effects. At large θ, the two fluids just flow past each other in opposite directions with little transverse mixing: after the fronts of the light and heavy fluid have reached respectively the top and bottom ends of the pipe, these start to fill up the corresponding tube sections. One finally reaches a state in which the light and heavy fluids have swapped locations and are now in a gravitationally stable configuration with a narrow transition zone [Fig. 3(b)]. At lower θ, there is still a preferential upwards flow near the

top of the tube sections and a downwards flow near the bottom. However, transverse mixing is much stronger so that fluid reaching an end is a mixture of light and heavy fluid. In Fig. 3(a), for instance, the final concentration is almost constant along the tube with just a slight stabilizing gradient.

To conclude, our experimental results demonstrate the crucial influence of local transverse mixing on buoyancy driven mixing in a confined tube geometry and its strong dependence on θ (as also observed in other systems such as sedimenting suspensions). Increasing θ reduces transverse mixing due to buoyancy forces across the tube section stabilising the interface between the fluids. There results a transition between macroscopically diffusive (large transverse exchange) and stable counterflow (weak exchange) regimes. Buoyancy forces across the tube also account for the strong increase of the macroscopic diffusion coefficient D with θ which contrasts with its weak dependence on At. Increasing the viscosity of the fluid both increases D and reduces the range of observation of the diffusive regime.

Unexpectedly, buoyancy driven mixing appears quite different in tilted tubes to vertical ones. Tilting the tube breaks the symmetry of flow: it tends to create counterflows of the two fluids with transverse exchange through Kelvin–Helmoltz instabilities. Tilting separates mixing and counterflow in the same way as Boycott effects separate particle sedimentation from backflow. This configuration is less complex than in vertical tubes where the relative concentration distribution varies randomly in the tube section with no preferential directions. Practically, tilting the tube allows one to obtain quickly very homogeneous mixtures for well chosen configurations. In order to understand better these phenomena and establish their scaling laws, the influence of more parameters, such as the tube diameter, will have to be investigated. Determining the characteristic time scales and velocities of the mixing processes will in addition require a quantitative analysis of the local concentration distributions and velocity fields.

We thank C. Saurine, G. Chauvin, C. Frenois, and R. Pidoux for realizing the experimental setup.

[1] M. H. I. Baird, K. Aravamudan, N. V. Rama Rao, J. Chadam, and A. P. Peirce, "Unsteady axial mixing by natural convection in vertical column," AIChE J. **38**, 1825 (1992).
[2] E. E. Zukoski, "A review of flows driven by natural convection in adiabatic shafts," NIST Report No. NIST-GCR-95-679 (1995), and references therein.
[3] G. K. Batchelor and J. M. Nitsche, "Instability of stationary unbounded stratified fluid," J. Fluid Mech. **227**, 357 (1991); "Instability of stratified fluid in a vertical cylinder," **227**, 419 (1991).
[4] D. H. Sharp, "An overview of Rayleigh–Taylor instability," Physica D **12**, 3 (1984).
[5] J. Fernandez, P. Kurowski, P. Petitjeans, and E. Meiburg, "Density driven, unstable flows of miscible fluids in a Hele-Shaw cell," J. Fluid Mech. **451**, 239 (2002).
[6] T. H. Ellison and J. S. Turner, "Turbulent entrainment in stratified flows," J. Fluid Mech. **6**, 423 (1959).
[7] T. J. Benjamin, "Gravity currents and related phenomena," J. Fluid Mech. **31**, 209 (1968).
[8] J. S. Turner, *Buoyancy Effects in Fluids* (Cambridge University Press, Cambridge, 1979).
[9] J. E. Simpson, *Gravity Currents in the Environment and the Laboratory*, 2nd ed. (Cambridge University Press, Cambridge, 1997).
[10] M. Debacq, V. Fanguet, J. P. Hulin, D. Salin, and B. Perrin, "Self-similar concentration profiles in buoyant mixing of miscible fluids in a vertical tube," Phys. Fluids **13**, 3097 (2001); M. Debacq, V. Fanguet, J. P. Hulin, D. Salin, B. Perrin, and E. J. Hinch, "Buoyant mixing of miscible fluids of varying viscosities in a vertical tube," *ibid.* **15**, 3846 (2003).
[11] A. Acrivos and E. Herbolzheimer, "Enhanced sedimentation in settling tanks with inclined walls," J. Fluid Mech. **92**, 435 (1979).
[12] E. Herbolzheimer, "Stability of the flow during sedimentation in inclined channels," Phys. Fluids **26**, 2043 (1983).
[13] G. A. Lawrence, F. K. Browand, and L. G. Redekopp, "The stability of the sheared density interface," Phys. Fluids A **3**, 2360 (1991).